Statistics of noninteracting many-body fermionic states
The question of a many-body mobility edge

Huang, Ke; Vu, DinhDuy; Das Sarma, Sankar; Li, Xiao

Published in:
Physical Review B

Published: 01/05/2024

Document Version:
Final Published version, also known as Publisher's PDF, Publisher's Final version or Version of Record

Published version (DOI):
10.1103/PhysRevB.109.174214

Publication details:
Huang, K., Vu, D., Das Sarma, S., & Li, X. (2024). Statistics of noninteracting many-body fermionic states: The question of a many-body mobility edge. *Physical Review B*, *109*(17), Article 174214. https://doi.org/10.1103/PhysRevB.109.174214

Huang, K., Vu, D., Das Sarma, S., & Li, X. (2024). Statistics of noninteracting many-body fermionic states: The question of a many-body mobility edge. *Physical Review B, 109(*17), Article 174214. https://doi.org/10.1103/PhysRevB.109.174214

Statistics of noninteracting many-body fermionic states: The question of a many-body mobility edge

Ke Huang,[1] DinhDuy Vu,[2,3] Sankar Das Sarma,[2] and Xiao Li[1,*]

[1]*Department of Physics, City University of Hong Kong, Kowloon, Hong Kong SAR, China*

[2]*Condensed Matter Theory Center and Joint Quantum Institute, University of Maryland, College Park, Maryland 20742, USA*

[3]*Department of Physics, Harvard University, Massachusetts 02138, USA*

(Received 22 June 2023; accepted 26 April 2024; published 31 May 2024)

In this work, we study the statistics of a generic noninteracting many-body fermionic system whose single-particle counterpart has a single-particle mobility edge (SPME). We first prove that the spectrum and the extensive conserved quantities follow the multivariate normal distribution with a vanishing standard deviation $\sim O(1/\sqrt{L})$ in the thermodynamic limit, regardless of SPME. Consequently, the theorem rules out an infinite-temperature or high-temperature many-body mobility edge (MBME) for generic noninteracting fermionic systems in any dimension. Further, we also prove that the spectrum of a one-dimensional fermionic many-body system with short-range interactions is qualitatively similar to that of a noninteracting many-body system up to the third-order moment. These results partially explain why neither short-range [Phys. Rev. B **107**, 035129 (2023)] nor long-range interacting systems exhibit an infinite-temperature MBME in a one-dimensional system.

DOI: 10.1103/PhysRevB.109.174214

I. INTRODUCTION

Strong disorder is a generic mechanism to create localized phases in both single-particle and many-body systems. In single-particle systems, strong disorder renders an extended system localized, a phenomenon known as Anderson localization [1]. Similarly, a many-particle system with strong disorder can become many-body localized (MBL) and avoid thermalization [2–7]. Roughly speaking, the extended and localized phases in the single-particle system "correspond" to the ergodic and the nonergodic phases in the many-body system. Beyond the extended and localized phases, the single-particle system can also have an intermediate phase with coexisting extended and localized eigenstates. In the intermediate phase, both the extended and localized states occupy a finite fraction of the whole spectrum. Furthermore, the two parts of the spectrum are energetically separated by the single-particle mobility edge (SPME) [8–16].

It is natural to ask what happens to the SPME when interparticle interactions are turned on: does it disappear, does it transform to something new and nontrivial, does the whole system thermalize, or does a new intermediate interacting phase or many-body mobility edge (MBME) emerge in between the thermal phase and the MBL phase? Many existing theoretical works on MBME [17–29] study whether there exists a critical energy in the many-body spectrum that separates MBL states from thermal ones. In other words, these works try to determine the critical temperature at which the system experiences the thermal-MBL transition. From a dynamical perspective, this amounts to determining whether randomly chosen initial states at different energies relax in a similar fashion. Hence, we call it the *finite-temperature MBME*, which has been found numerically and experimentally even in systems without SPME. To detect this type of MBME using quench experiments, one needs to start the experiment with initial states at different energies. However, this subject is controversial, as these results were mostly obtained in small systems, and some arguments [30] suggest that the finite-temperature MBME may not exist in the thermodynamic limit. In this context, it may be relevant to point out that MBL itself may not survive for large systems at long times [31,32].

If we push the temperature to infinity, the finite-temperature MBME becomes the *infinite-temperature MBME*. Physically, this means that the MBME appears precisely at the peak of the many-body density of states (DOS), the energy of which we denote as ε_c.[1] Meanwhile, the DOS is narrowly peaked around ε_c in a many-body spectrum. As a result, there will be a finite portion of eigenstates below and above the infinite-temperature MBME. Therefore such an infinite-temperature MBME always implies the existence of a finite portion of both MBL and thermal states in the many-body spectrum. This is in contrast to the finite-temperature MBME, which, depending on the temperature, is typically shifted away from ε_c by more than the width of the many-body DOS. Consequently, in a system with a finite-temperature MBME, MBL or thermal states may become a minority in the spectrum. To measure this type of MBME, we note that it constitutes one possible scenario of an infinite-temperature many-body intermediate phase (which contains a mixture of MBL and thermal eigenstates). Therefore one can conduct a quench experiment starting with random initial states (without controlling their energies) and then observe whether the system exhibits different relaxation dynamics as the disorder strength varies [33]. Curiously, such an infinite-temperature MBME has not been observed in the experiment.

Our previous work [34] specifically studied the t_1-t_2 model (which has an SPME) with short-range (SR) interactions,

*xiao.li@cityu.edu.hk

[1]For a precise definition of ε_c please refer to Eq. (20).

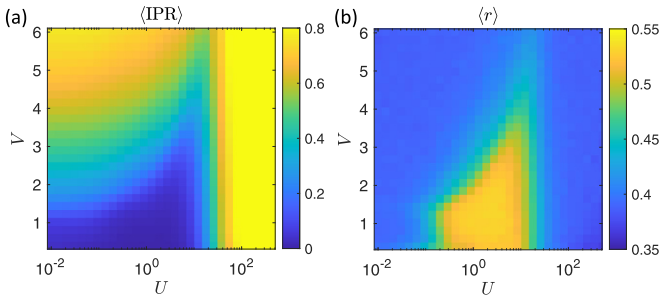

FIG. 1. (a) IPR and (b) mean gap ratio of the t_1-t_2 model with long-range interaction. Here, we take $t_2 = 1/6$, and the system size is $L = 16$. The results are averaged over six random phases.

in which the SPME does not induce an infinite-temperature MBME, though the signature of MBME at low temperatures has been found in small systems. In the current work, we first analyze the t_1-t_2 model with long-range (LR) interactions, which turns out to be qualitatively similar to the SR interaction case for intermediate interacting strength and has no infinite-temperature MBME as well. Thus we go back to the noninteracting model to see whether the ineffectiveness of the SPME in inducing an MBME is a consequence of interaction at all, or whether it arises from some intrinsic single-particle properties. We do this by studying the noninteracting many-body fermionic system.

Note that a recent work [35] introduced a numerical algorithm to obtain the exact DOS in finite-size noninteracting systems efficiently. In this work, however, we focus on the statistical behavior in the thermodynamic limit. Though the thermal-MBL transition at a generic (finite) temperature is a rather difficult problem, we can establish at high and infinite temperatures that, for noninteracting fermions, the DOS and other extensive quantities commuting with the Hamiltonian form a multivariate normal distribution with parameters determined by the expectation value and the variance of the single-particle system. This theorem implies that all detailed structures in the single-particle spectrum, including the SPME, are smeared in the many-body system. Moreover, the standard deviation of the many-body energy eigenvalues scales as $O(1/\sqrt{L})$. Therefore the DOS in the thermodynamic limit is zero almost everywhere in the many-body system. This is in stark contrast to the single-particle case, where the DOS is spread over the whole spectrum. Further, the energy-resolved standard deviation of extensive quantities also manifests the $O(1/\sqrt{L})$ scaling, which precludes both the infinite- and high-temperature MBME in noninteracting fermionic systems. Finally, we analyze the effect of the SR interaction on the noninteracting spectrum. Limited to small system sizes, the numerical results suggest that the many-body spectrum of the interacting system has a broader width and a finite skewness, signifying an asymmetry. However, we demonstrate that these are finite-size effects, as we show that up to the third-order moment, the spectrum of the interacting systems also follows the $O(1/\sqrt{L})$ scaling.

The structure of the paper is the following. In Sec. II, we analyze the effect of the LR interaction in the t_1-t_2 model, demonstrating that no infinite-temperature MBME emerges in the numerical results. In Sec. III, we present the central result of this work. Specifically, we show that due to the central limit theorem (CLT), most details in the single-particle spectrum are washed out when we build the many-body states. This result explains why the SPME is ineffective in inducing the infinite- and high-temperature MBME. In Sec. IV, we analyze how short-range interactions modify the spectrum of a noninteracting fermionic system. Finally, in Sec. V, we provide additional discussions and conclude this paper.

II. LONG-RANGE INTERACTION

In this section, we consider the t_1-t_2 model with LR interaction at half-filling, given by

$$H = \sum_j (t_1 c_j^\dagger c_{j+1} + t_2 c_j^\dagger c_{j+2} + \text{H.c.}) + \sum_j V_j n_j + \frac{1}{2}\sum_{i\neq j} U_{|i-j|} n_i n_j, \tag{1}$$

where $V_j = V\cos(2\pi q j + \phi)$ is the quasiperiodic potential with $q = (\sqrt{5}-1)/2$, and ϕ is a random phase. Here, we adopt the periodic boundary condition and study the Coulomb interaction given by

$$U_r = U\left(\frac{L}{\pi}\sin\frac{\pi r}{L}\right)^{-1}. \tag{2}$$

Additionally, we set $t_1 = 1$ as the energy unit and take $t_2 = 1/6$.

To quantify the localization transition of the many-body eigenstates, we utilize the many-body inverse participation ratio (MIPR), defined as [36]

$$\mathcal{I} = \frac{1}{1-N/L}\left[\frac{1}{N}\sum_{i=1}^{L}\bar{n}_i^2 - N/L\right], \tag{3}$$

where N is the total particle number, and $\bar{n}_i$ is the particle number expectation value on site i. The MIPR describes the density distribution in real space, and we have $\mathcal{I} \to 0$ for an extended state, while $\mathcal{I} \to 1$ for a localized state. In Fig. 1(a), we calculate the MIPR of the t_1-t_2 model in a system of length $L = 16$, which exhibits qualitatively similar behavior as the Aubry-André (AA) model and the Anderson model with LR interactions [36]. Specifically, the t_1-t_2 model with LR interaction possesses three distinct regimes for different interaction strengths: the single-particle regime $U \ll O(1)$, the many-body regime $U \sim O(1)$, and the Mott regime $U \gg O(1)$. Compared with the t_1-t_2 model with SR interaction [34], the LR interaction manifests no qualitative difference in the single-particle and the many-body regimes. However, the LR interaction fundamentally alters the Hilbert space structure in the Mott regime, resulting in localization at infinitesimal disorder strengths.

We also calculate the mean gap ratio to characterize the thermal-MBL transition. The gap ratio is defined by [37,38]

$$r_i = \min\left\{\frac{\delta E_i}{\delta E_{i+1}}, \frac{\delta E_{i+1}}{\delta E_i}\right\}, \tag{4}$$

where $\delta E_i = E_{i+1} - E_i$ is the energy gap between two adjacent eigenenergies. In the thermal phase, the spectrum follows the Gaussian orthogonal ensemble (GOE) whose mean gap

ratio $\langle r\rangle$ is 0.53, whereas the spectrum follows the Poisson distribution in the MBL phase with $\langle r\rangle = 0.386$. As shown in Fig. 1(b), the interaction range has no significant effect in the single-particle and the many-body regimes. However, the thermal Mott regime for the SR interaction disappears in the presence of the LR interaction. This phenomenon is subtly different from the corresponding situation in the AA model and the Anderson model, which are not thermal in the Mott regime for the SR interaction because of the Hilbert-space fragmentation [36,39,40]. The similarity between SR and LR cases in the many-body regime suggests that the LR interaction cannot induce a many-body intermediate phase arising from the single-particle intermediate phase.

Finally, the thermal-MBL transition can also be identified by studying the spectral form factor. We have included such results in Appendix C.

III. NONINTERACTING FERMIONS

In this section, we analyze the statistical properties of noninteracting many-body fermionic states. We will discuss three questions. In Sec. III A, we introduce a revised central limit theorem (CLT) for noninteracting fermions. In Sec. III B, we use this result to argue that the MIPR must be a continuous function of energy, which rules out the infinite- and high-temperature MBME in a noninteracting fermionic system. Finally, in Sec. III C, we show that the MIPR in a half-filled fermionic system must be an even function of energy.[2]

A. Revised central limit theorem for noninteracting fermions

Our previous work has shown that neither SR nor LR interactions could introduce an MBME in the interacting t_1-t_2 model [34]. This suggests that the SPME does not generally give rise to MBME in an interacting many-body system. Therefore the ineffectiveness of the SPME in introducing an MBME in the many-body system may not be caused by the interaction. Hence, we take a step back and study the noninteracting many-body system. In a noninteracting classical system with no indistinguishability, each particle can be regarded as an independent variable. Hence, the statistics of an extensive quantity $X_{\rm tot} = \sum_{i=1}^{N} X_i$ follows the CLT

$$\frac{X_{\rm tot} - \mu_x N}{\sqrt{N}\sigma_x} \sim \mathcal{N}(0,1), \tag{5}$$

where X_i is the extensive quantity of particle i, μ_x and σ_x^2 are the expectation value and the variance of X_i, and $\mathcal{N}(\mu,\sigma^2)$ is the univariate normal distribution with mean μ and standard deviation σ. For instance, if X_i is the energy of a particle, the CLT implies that the density of states of the many-body spectrum is a Gaussian function.

However, the CLT does not apply to fermionic systems, as the Pauli exclusion principle implies that particles are not independent variables. In fact, building a many-body state in a fermionic system is equivalent to sampling without replacement. If a quantity X of orbital i takes value x_i and there are L orbitals, then calculating $X_{\rm tot}$ of N particles amounts to choose N samples out of L objects. Further, we must deal with the multivariate distribution if there are multiple quantities. Hence, we can ask whether there is a revised CLT for a noninteracting many-body fermionic system where all the variables are not independent.

To begin with, we consider the case with just two variables. Suppose that we have two sets of values $X = \{x_i\}_{i=1}^{L}$, $Y = \{y_i\}_{i=1}^{L}$, and $\{X_j\}_{j=1}^{N}$, $\{Y_j\}_{j=1}^{N}$ $(N < L)$ are the random variables representing the sampling without replacement. Because of the permutation symmetry, we know that the probability $P(X_j = x_i) = P(X_1 = x_1) = 1/L$ and that $P(X_j = x_i | X_k = x_l) = (1-\delta_{il})/(L-1)$ if $j \neq k$. As a result, the expectation value of $(X_j - \mu_x)(X_k - \mu_x)$ is

$$\begin{aligned}
&\mathbb{E}[(X_j-\mu_x)(X_k-\mu_x)] \\
&= \sum_{i=1}^{L}(x_i-\mu_x)P(X_j=x_i)\cdot\sum_{l=1}^{L}(x_l-\mu_x)P(X_k=x_l|X_j=x_i) \\
&= \frac{1}{L(L-1)}\sum_{i\neq l}(x_i-\mu_x)(x_l-\mu_x) \\
&= \frac{1}{L(L-1)}\left[\left(\sum_i x_i-\mu_x L\right)^2-\sum_i(x_i-\mu_x)^2\right] \\
&= \frac{\sigma_x^2}{L-1}.
\end{aligned} \tag{6}$$

Consequently, we have

$$\mathbb{E}(X_{\rm tot}-\mu_x N)^2 = \frac{N(L-N)}{L-1}\sigma_x^2. \tag{7}$$

Similarly, we have

$$\mathrm{Cov}(X_{\rm tot}, Y_{\rm tot}) = \frac{N(L-N)}{L-1}\mathrm{Cov}(X,Y), \tag{8}$$

where $\mathrm{Cov}(X,Y)$ is the covariance between X and Y.

More generally, we prove in Appendix A that all the moments agree with those of the multivariate normal distribution in the thermodynamic limit. This implies that if Σ, the covariance matrix between X and Y, is positive definite, we have

$$\frac{X_{\rm tot}-\mu_x N}{\sqrt{\nu(1-\nu)L}}, \frac{Y_{\rm tot}-\mu_y N}{\sqrt{\nu(1-\nu)L}} \sim \mathcal{N}(0,\Sigma), \tag{9}$$

where $\mathcal{N}(0,\Sigma)$ denotes the multivariate normal distribution, and $\nu = N/L$ is the filling factor. We emphasize that Eq. (9) does not depend on the dimension of the system. Note that the univariate case of the above result has been proven in Ref. [41]. In Fig. 2, we present a numerical example of this CLT. In the right panel, we set $L = 1000$, $N = 300$, and take either $Y = \cos(X)$ or $Y = \sin(X)$, which agrees perfectly with the normal distribution $\mathcal{N}(0,\Sigma)$ shown in the left panel. Here, the value of x_i is generated by the normal distribution, and, as we cannot obtain all the product states, we randomly choose 10^6 product states (with replacement) as the sample.

A crucial implication of Eq. (9) is that the conditional expectation of $Y_{\rm tot}$ depends on $X_{\rm tot}$ linearly. In particular, we have

$$\mathbb{E}(Y_{\rm tot}|X_{\rm tot}=x) = \frac{\mathrm{Cov}(X,Y)}{\sigma_x^2}(x-\mu_x N)+\mu_y N, \tag{10}$$

[2]We always set the mean energy of the single-particle system as zero in this work.

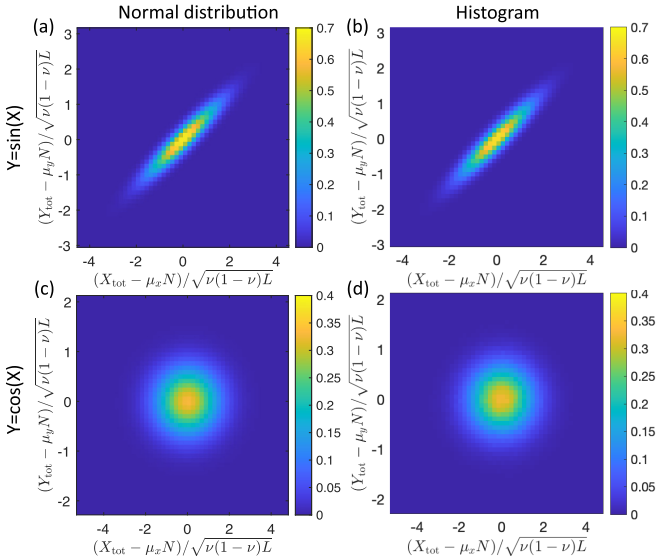

FIG. 2. The normal distribution predicted by CLT (left panel) and the histogram of $X_{\rm tot}, Y_{\rm tot}$ (right panel). Further, we consider the antisymmetric case $Y = \sin(X)$ in the upper panel, and the symmetric case $Y = \cos(X)$ in the lower panel.

whose generic behavior is shown in Fig. 2(a). Further, if $Y = f(X)$ and f is an even function, $\mathrm{Cov}(X, Y) = 0$ and therefore $X_{\rm tot}, Y_{\rm tot}$ are independent. Hence, the conditional expectation is constant. This special case is shown in Fig. 2(c), where the highlighted region has a circular shape.

Furthermore, Eq. (9) also suggests the equivalence of the microcanonical ensemble and the canonical ensemble at high temperatures. We first consider the infinite temperature case, where the system is controlled by the DOS of the many-body spectrum. We take $X_{\rm tot}$ to be the total energy, and thus we have the analytic expression of the DOS, given by

$$g(\varepsilon) \propto \exp\left[-\frac{N}{2}\frac{(\varepsilon-\mu_\varepsilon)^2}{\sigma_\varepsilon^2(1-\nu)}\right], \tag{11}$$

where $\varepsilon = E/N$ is the energy per particle. Note that the energy per particle is equivalent to the energy density up to a linear transformation, and the latter has been used extensively in the studies of MBME [17–29]. Therefore, in the thermodynamic limit, almost all the states reside in a small energy interval centered at μ_ε of width $O(1/\sqrt{N})$, which is essentially the microcanonical ensemble.

At any finite temperature, the density matrix of the canonical ensemble is given by

$$\rho = \frac{e^{-\beta H}}{\mathrm{tr}[e^{-\beta H}]} \propto \int \mathrm{d}\varepsilon |\varepsilon\rangle\langle\varepsilon| e^{-\beta N\varepsilon} g(\varepsilon), \tag{12}$$

where β is the inverse temperature. Thus, in the high-temperature limit ($\beta\sigma_\varepsilon \ll 1$), we obtain

$$e^{-\beta N\varepsilon} g(\varepsilon) \propto \exp\left[-\frac{N}{2}\frac{(\varepsilon-\tilde{\mu}_\varepsilon)^2}{\sigma_\varepsilon^2(1-\nu)}\right], \tag{13}$$

where $\tilde{\mu}_\varepsilon = \mu_\varepsilon - \beta(1-\nu)\sigma_\varepsilon^2$. Hence, the finite temperature just means shifting the center of the energy interval from μ_ε to $\tilde{\mu}_\varepsilon$, and the canonical ensemble is still equivalent to the microcanonical ensemble in this case.

B. The energy dependence of MIPR

We now use the above revised CLT to argue that the MIPR must be a continuous function of energy, which rules out the infinite- and high-temperature MBME in a noninteracting fermionic system. To start, note that the extent of localization in a single-particle system can be measured by the single-particle IPR (SIPR) defined by

$$I_s = \frac{L\sum_j |\psi_j|^4 - 1}{L-1}, \tag{14}$$

where ψ_j is the wave function on site j. SIPR vanishes in the thermodynamic limit unless the state is localized. For a generic noninteracting system, where the many-body eigenstates are all product states, we can introduce the mean SIPR (m-SIPR) of a many-body eigenstate, defined as the mean IPR of its constituent single-particle orbitals. Hence, the m-SIPR is an extensive quantity, and therefore, we can apply Eq. (9) to the bivariate distribution of the energy and the m-SIPR. What is more, if the SIPR is an even function of energy, the m-SIPR is independent of the energy. However, as long as there is a finite covariance between the SIPR and the energy, the m-SIPR will vary linearly with the energy, regardless of whether an SPME exists in the single-particle model. Furthermore, the energy-resolved standard deviation of the m-SIPR (i.e., the standard deviation of the m-SIPR within a small energy window) also scales as $O(1/\sqrt{L})$ because of the CLT. Hence, in the thermodynamic limit, almost all states within a small energy window have similar properties. Notwithstanding, as MIPR has no additivity, Eq. (9) does not apply to MIPR. However, the MIPR and the m-SIPR are not irrelevant, as they have the same mean value averaged over all many-body eigenstates [36]. The numerical results in Fig. 3 indeed show the similarity between the MIPR and the m-SIPR.

As the CLT scales as $O(1/\sqrt{L})$, one really needs a large system for the results to be definitive. Particularly, we consider the noninteracting t_1-t_2 model of $L = 144$ at half filling in Fig. 3, and study two cases, one with an SPME and the other without, as shown in Figs. 3(a) and 3(e). Similar to Fig. 2, we randomly choose 10^6 product states as the sample (with replacement). Because of the CLT, almost all the states concentrate within a small energy window compared with the whole spectrum, which can be observed in Figs. 3(d) and 3(h). Within that window, we compute the energy-resolved averaged m-SIPR and MIPR in Figs. 3(b) and 3(f). We have several observations. First, the m-SIPR agrees perfectly with Eq. (10). Second, not only is the MIPR symmetric relative to the spectral center, but it is also more uniform than the m-SIPR. Third, the energy-resolved standard deviation of both m-SIPR and MIPR is very small and follows the $O(1/\sqrt{L})$ scaling as shown in Figs. 3(c) and 3(g), suggesting that eigenstates within the same energy window have similar localization properties.

From the above observations, we conclude that in a large but finite system, only two degrees of freedom of the single-particle system—the mean value and the variance—play a role in the corresponding noninteracting many-body system.

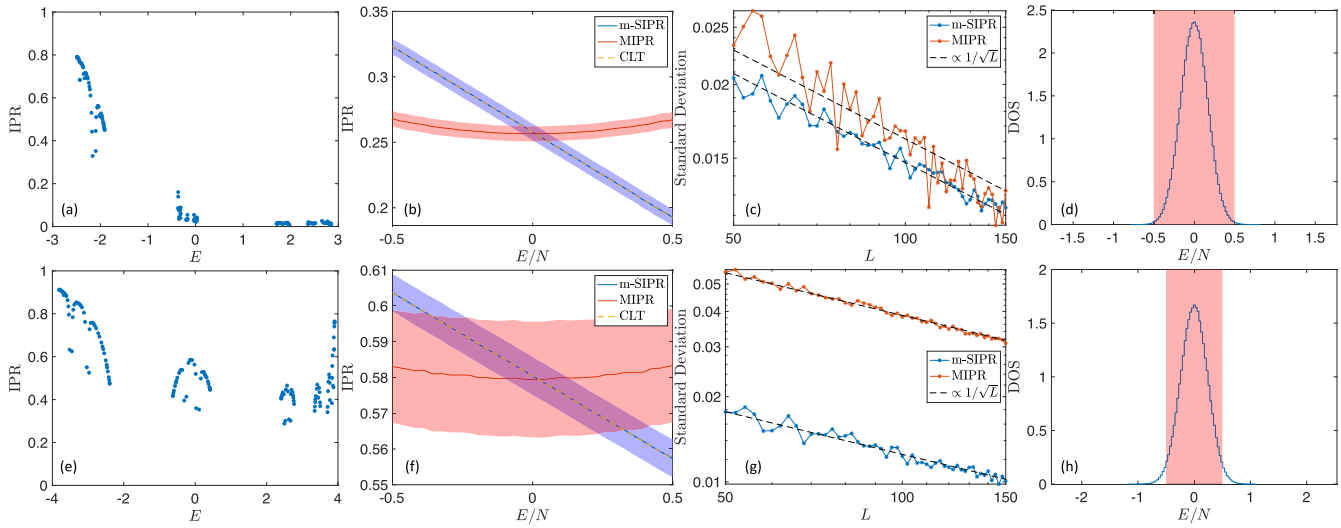

FIG. 3. [(a)–(d)] t_1-t_2 model with $V = 2$ (where SPME exists). [(e)–(h)] t_1-t_2 model with $t_2 = 1/6$, $V = 3.5$ (where no SPME exists). (a) and (e) plot the SIPR of the single-particle eigenstates. (b) and (f) show the energy-resolved average m-SIPR and average MIPR of the many-body eigenstates at half filling, and the shaded area indicates the standard deviation of the corresponding IPR around each energy. In addition, the dashed lines are the CLT predictions given by Eq. (10). (c) and (g) plot the standard deviation of the energy-resolved m-SIPR and MIPR for various system sizes. The calculation is done for 5% of the sampling states around the spectral center, and the black dashed lines are the fittings. (d) and (h) plot the DOS at half filling. The range of the horizontal axis in (d) and (h) represents the range of the entire energy spectrum, while the shade range is the energy range used in (b) and (f).

Moreover, even the variance has no effect in the thermodynamic limit because of the $O(1/\sqrt{L})$ scaling. Additionally, given that the m-SIPR varies smoothly with energy and that a finite high temperature is equivalent to a shift in the center of the spectrum [see Eq. (13)], we conclude that noninteracting many-body systems have neither infinite-temperature MBME nor high-temperature MBME. The fact that the noninteracting system itself does not manifest an MBME, despite perhaps having a single-particle mobility edge, provides a strong hint that there may not be any MBME in the corresponding interacting system.

C. MIPR in a half-filled system

In Fig. 3, we observed that the plotted MIPR is an even function of energy. Actually, this is not a coincidence. This feature arises from two crucial properties of a noninteracting many-body system at half-filling. The first is that any product state and its complement (under particle-hole operation) must have opposite energies. The second is that any product state and its complement have the same MIPR.

The first property is easy to understand. If a product state occupies half of the orbitals, its complementary state will occupy the rest of the orbitals. As a result, the energy of the product state and its complement will have opposite energies. To establish the second property, we first need to prove the following identity,

$$\langle n_i\rangle_\psi + \langle n_i\rangle_{\psi_c} = 1, \tag{15}$$

where n_i is the particle number and $|\psi_c\rangle$ is the complement of $|\psi\rangle$. Suppose that $|\psi\rangle = \prod_{i\in\Omega} f_i^\dagger |\text{vac}\rangle$, where $f_j = \sum_k U_{jk} c_k$, with c_k being the annihilation operator on site k. We then have $|\psi_c\rangle = \prod_{i\in\Omega^c} f_i^\dagger |\text{vac}\rangle$, where Ω_c is the complement of Ω. Therefore

$$\langle n_i\rangle_\psi = \sum_{j,k\in\Omega} U_{ij}^* U_{ik} \langle f_j^\dagger f_k\rangle_\psi = \sum_{j,k\in\Omega} U_{ij}^* U_{ik}\delta_{jk} = \sum_{j\in\Omega} |U_{ij}|^2. \tag{16}$$

Hence, we obtain

$$\langle n_i\rangle_\psi + \langle n_i\rangle_{\psi_c} = \sum_{j\in\Omega} |U_{ij}|^2 + \sum_{j\in\Omega^c} |U_{ij}|^2 = 1,$$

where the last equality follows from the unitarity of U_{ij}. Following this, we derive

$$\begin{aligned}\sum_{i=1}^{L} (\bar{n}_i)_c^2 &= \sum_{i=1}^{L} (1-\bar{n}_i)^2 \\ &= \sum_{i=1}^{L} 1 - 2\sum_{i=1}^{L} \bar{n}_i + \sum_{i=1}^{L} \bar{n}_i^2 = \sum_{i=1}^{L} \bar{n}_i^2,\end{aligned} \tag{17}$$

where $\bar{n}_i$ and $(\bar{n}_i)_c$ denotes the expectation on $|\psi\rangle$ and $|\psi_c\rangle$ respectively, and we use $\sum_{i=1}^{L} \bar{n}_i = L/2$ for the last equality. Therefore these two states have exactly the same MIPR. This result may seem counterintuitive because if exactly half of the orbitals are extended and half localized, then the product state of the extended states has the same MIPR as that of the localized states. However, one should not simply infer the property of a product state from a specific basis. An example is that the product state of a completely filled band (extended) is the same as that of their Wannier functions (localized). Therefore, even if the low-energy orbitals are extended while the high-energy orbitals are localized, the low-energy many-body states are as localized as their high-energy counterparts.

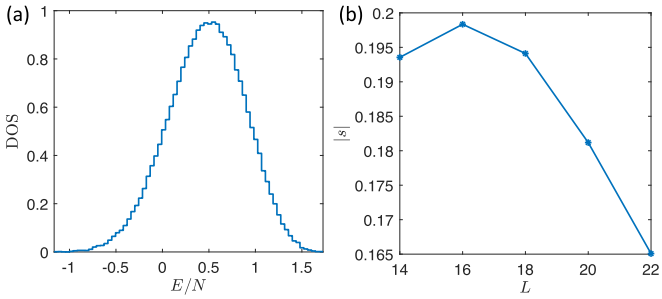

FIG. 4. (a) DOS of the t_1-t_2 model with $L = 18$. (b) Skewness of the spectrum for various system sizes. Here, we take $t_2 = 1/6$, and $V = U = 1$.

IV. FERMIONS WITH SHORT-RANGE INTERACTION

Having understood the properties of noninteracting fermions, a natural question is how the spectrum of a noninteracting many-body fermionic system is modified by the interactions. Here we specifically study the t_1-t_2 model with the nearest-neighbor interaction in [34], $U_r = U\delta_{r,1}/2$. In Fig. 4(a), we calculate the DOS in a system of $L = 18$ by exact diagonalization. It has two distinct features compared with the DOS in the noninteracting spectrum. First, the DOS is now an asymmetric function of energy, quantified by a nonzero skewness defined as

$$s = \frac{\langle (H - \langle H\rangle)^3\rangle}{[\langle H^2\rangle - \langle H\rangle^2]^{\frac{3}{2}}}, \tag{18}$$

where $\langle \mathcal{O}\rangle \equiv \mathrm{tr}\{\mathcal{O}\}/D$ denotes the trace of $\mathcal{O}$ divided by the Hilbert space dimension D. As shown in Fig. 4(b), the skewness shows no clear scaling relation for numerically accessible system sizes. Second, the width of the DOS is much broader than that of the noninteracting results in Figs. 3(d) and 3(h).

However, we can show that both features are finite-size effects. In particular, we prove in Appendix B that

$$\lim_{L\to\infty}\left\langle\left(\frac{H-\varepsilon_c N}{\sqrt{L}}\right)^2\right\rangle = \sigma_\varepsilon^2\nu(1-\nu) + U^2\nu^2(1-\nu)^2,$$
$$\lim_{L\to\infty}\left\langle\left(\frac{H-\varepsilon_c N}{\sqrt{L}}\right)\right\rangle = \lim_{L\to\infty}\left\langle\left(\frac{H-\varepsilon_c N}{\sqrt{L}}\right)^3\right\rangle = 0. \tag{19}$$

In the above equation, ε_c is the *peak of the many-body DOS*, defined as

$$\varepsilon_c \equiv \lim_{L\to\infty}\frac{\langle H\rangle}{N} = \mu_\varepsilon + \nu U, \tag{20}$$

where μ_ε is the single-particle mean energy (equivalent to the mean energy of the noninteracting many-body Hamiltonian). Here, the result is based on the NN interaction in one dimension, and thus, the behavior could be different in higher dimensions.

The above result indicates that the interacting system also possesses a $1/\sqrt{L}$ scaling, similar to the noninteracting case. Hence, in the thermodynamic limit, all states are concentrated within a small energy window centered at $E = \varepsilon_c N$, indicating that the infinite-temperature canonical ensemble for an interacting system is equivalent to the microcanonical ensemble at $E = \varepsilon_c N$. By analogy with the noninteracting case, we conjecture that a finite high temperature is equivalent to shifting the energy of the microcanonical ensemble. This indicates that the infinite-temperature MBME, even if it exists, can only occur at $E/N = \varepsilon_c + O(1/\sqrt{N})$. Moreover, the vanishing skewness of the spectrum suggests that the DOS in a large system would be more symmetric than that in a small system. Hence, up to the third-order moment, the spectrum of a system with SR interactions is qualitatively similar to that of a noninteracting system in the thermodynamic limit. Note that we do not study LR interactions in this section because we do not have an analytical result like Eq. (19) for LR interactions. Hence, LR interactions may possess a different scaling behavior.

V. DISCUSSION AND CONCLUSION

The question of what happens to the single-particle mobility edge separating low-energy localized states from the high-energy extended states in the single-particle spectrum of various well-studied noninteracting quasiperiodic models in the presence of interparticle interactions has remained controversial and open. In particular, there is limited numerical evidence in small-system studies that the SPME in the noninteracting system leads to an MBME in the interacting many-body spectrum in the presence of interactions. It is also possible that interactions destroy the SPME, and the interacting many-body spectrum does not manifest any MBME. We address this important question with a new approach, where we study the noninteracting many-body spectrum for fermions, establishing that even the many-body noninteracting spectrum does not manifest any MBME, although the corresponding single-particle spectrum manifests an SPME. This strongly suggests that there is no infinite- and high-temperature MBME for interacting systems whose noninteracting counterparts have SPMEs.

We provide further support for this conclusion by explicitly studying interacting one-dimensional quasiperiodic models, which are known to have noninteracting SPMEs in the single-particle spectra. Specifically, we study the t_1-t_2 model with LR interaction, extending the previous work on the SR interacting model [34] to establish that an infinite-temperature MBME cannot generally emerge from the SPME regardless of the type (LR or SR) of interaction. In fact, we demonstrate that the SPME has no qualitative effect on the many-body spectrum, even without any interaction. We understand this result by resorting to the CLT, which dictates that the multivariate distribution of the energy and the other extensive quantities commuting with the Hamiltonian follows the multivariate normal distribution. Thus the CLT obscures and suppresses most details in the single-particle spectrum, including the SPME. Moreover, the standard deviation of the spectrum and the energy-resolved standard deviation of the extensive quantities follow the $O(1/\sqrt{L})$ scaling imposed by the CLT. As a result, the noninteracting fermionic many-body system generally has neither an infinite-temperature MBME nor a high-temperature MBME. Furthermore, we also prove that the spectrum of the SR interacting systems still follows the $O(1/\sqrt{L})$ system-size scaling up to the third-order moment, although the numerical results in small systems may not exhibit this feature clearly. Hence, the finite-temperature MBME does not imply the infinite-temperature many-body intermediate phase in

both SR interacting and noninteracting systems. However, we emphasize that the multivariate distribution of the energy and the MIPR may no longer follow the same $O(1/\sqrt{L})$ scaling in the presence of interactions, which could differentiate the thermal and MBL phases.

To summarize, there are four important results in this work. First, we establish the multivariate CLT in the noninteracting fermionic systems. The CLT shows that the distribution only depends on two statistical quantities of the single-particle system: the mean value and the covariance. Second, the CLT obscures and suppresses most details in the single-particle spectrum, including the SPME, which precludes the infinite- and high-temperature MBME in noninteracting many-body systems. Third, we extend the above results to models with SR interactions, which have the same scaling law as noninteracting systems up to the third-order moment of the energy. Thus we show that both the variance and the skewness of the energy (the width and the asymmetry of the DOS) vanish in the thermodynamic limit. Finally, we show that for both noninteracting and SR interacting systems, the DOS is highly concentrated around its peak value. Hence, a finite-temperature MBME does not imply an infinite-temperature many-body intermediate phase. Our work strongly hints that there is unlikely to be any MBME in an interacting many-body spectrum, independent of whether the corresponding single-particle noninteracting system has an SPME.

ACKNOWLEDGMENTS

This work is supported by the Laboratory for Physical Sciences. X.L. also acknowledges support from the National Natural Science Foundation of China (Grant No. 11904305), the Research Grants Council of Hong Kong (Grants No. CityU 21304720, No. CityU 11300421, No. CityU 11304823, and No. C7012-21G), as well as City University of Hong Kong (Project No. 9610428). K.H. is supported by the Hong Kong PhD Fellowship Scheme.

APPENDIX A: CENTRAL LIMIT THEOREM FOR NONINTERACTING FERMIONS

Suppose the noninteracting Hamiltonian H of system size L and another observable Q commuting with the Hamiltonian are given by

$$H=\sum_{i=1}^{L}\varepsilon_i n_i,\quad Q=\sum_{i=1}^{L}q_i n_i. \tag{A1}$$

For the following discussion, we also assume that $\lim_{L\to\infty}\frac{1}{L}\sum_{i=1}^{L}\varepsilon_i^m$ and $\lim_{L\to\infty}\frac{1}{L}\sum_{i=1}^{L}q_i^m$ exist for all positive integer m and that

$$\begin{aligned}&\lim_{L\to\infty}\frac{N}{L}=\nu>0,\quad \lim_{L\to\infty}\frac{1}{\sqrt{L}}\sum_{i=1}^{L}q_i=0,\quad \lim_{L\to\infty}\frac{1}{\sqrt{L}}\sum_{i=1}^{L}\varepsilon_i=0,\\ &\lim_{L\to\infty}\frac{1}{L}\sum_{i=1}^{L}\varepsilon_i^2=\sigma_\varepsilon^2>0,\quad \lim_{L\to\infty}\frac{1}{L}\sum_{i=1}^{L}q_i^2=\sigma_q^2>0,\quad \lim_{L\to\infty}\frac{1}{L}\sum_{i=1}^{L}\varepsilon_i q_i=0.\end{aligned} \tag{A2}$$

Note that ε_i, q_i and N are all functions of L implicitly. Additionally, we also know that $\lim_{L\to\infty}\frac{1}{L}\sum_{i=1}^{L}\varepsilon_i^m q_i^n$ exists because of the Cauchy inequality. Further, we introduce the following p-tuple moment for $x=(x_1,x_2,\cdots,x_p)$

$$f(x)=\sum_{p}{}'\varepsilon_{i_1}^{x_1}\varepsilon_{i_2}^{x_2}\cdots\varepsilon_{i_p}^{x_p}, \tag{A3}$$

where x_j are all positive integers, and $\sum_p{}'$ denotes $\sum_{\substack{1\leqslant i_1,i_2,\cdots,i_p\leqslant L\\ \text{all different}}}$. First, we have

$$\begin{aligned}f(x)=&f(x_1,x_2,\cdots,x_{p-1})f(x_p)\\ &-\sum_{j=1}^{p-1}f(x_1,\cdots,x_i+x_p,\cdots,x_{p-1}),\end{aligned} \tag{A4}$$

because

$$\sum_{p-1}{}'\sum_{1\leqslant i_p\leqslant L}=\sum_{p}{}'+\sum_{p-1}{}'\sum_{k=1}^{p-1}\delta_{i_p,i_k}. \tag{A5}$$

Next, we are going to prove that $\lim_{L\to\infty}f(x)L^{-|x|/2}$ always exists, where $|x|=\sum_{j=1}^{p}x_j$. For 1-tuples, this statement holds true because of Eq. (A2). If the statement holds for $(p-1)$-tuples, then for p-tuple x, we have

$$\lim_{L\to\infty}\frac{f(x)}{L^{|x|/2}}=\lim_{L\to\infty}\frac{f(x')}{L^{|x'|/2}}\cdot\frac{f(x_p)}{L^{|x_p|/2}}-\lim_{L\to\infty}\sum_{j=1}^{p-1}\frac{f(x_j')}{L^{|x|/2}}, \tag{A6}$$

where $x'=(x_1,x_2,\cdots,x_{p-1})$, and $x_j'=(x_1,\cdots,x_j+x_p,\cdots,x_{p-1})$. Here, we used the fact $|x_j'|=|x|$. As x' and x_j' are all $(p-1)$-tuples, the RHS of Eq. (A6) exists, and therefore the LHS also exists. A direct corollary is that $\lim_{L\to\infty}f(x)L^{-|x|/2}=0$ if $\max\{x\}\geqslant 3$. First, $\lim_{L\to\infty}f(x_1)L^{-|x_1|/2}=0$ if $x\geqslant 3$. If it holds for $(p-1)$-tuples, then for p-tuple x with $\max\{x\}\geqslant 3$, we also have Eq. (A6). Without loss of generality, we suppose $x_p\geqslant 3$, and then $\max\{x_j'\}\geqslant x_j+x_p\geqslant 3$. Thus all $(p-1)$-tuples x_j' satisfies $\lim_{L\to\infty}f(x_j')L^{-|x|/2}=0$, and so does the p-tuple x. It can be proved similarly that $\lim_{L\to\infty}f(x)L^{-|x|/2}=0$ if $|x|$ is odd.

We denote the trace divided by dimension in the fixed particle number subspace as $\langle\cdot\rangle$. Obviously, for all different $i_1,i_2,\ldots,i_p$, we have

$$\langle p\rangle\equiv\langle n_{i_1}n_{i_2}\cdots n_{i_p}\rangle=\langle n_1n_2\cdots n_3\rangle=\frac{N!/(N-p)!}{L!/(L-p)!}. \tag{A7}$$

Whereby, we know $\lim_{L\to\infty}\langle n_{i_1}n_{i_2}\cdots n_{i_p}\rangle = \nu^p$. Hence, we know that $\lim_{L\to\infty}\frac{\langle H^{2m+1}\rangle}{L^{m+1/2}} = 0$. For H^{2m}, we have

$$H^{2m} = \sum_{p=1}^{2m}\sum_{\substack{x_1\geqslant\cdots\geqslant x_p\geqslant 1\\ |x|=2m}} c(x)\sum_{p}{}'\prod_{j=1}^{p}\varepsilon_{i_j}^{x_j}\prod_{j=1}^{p} n_{i_j}, \tag{A8}$$

where $c(x)$ is some integer coefficient for p-tuple x. For convenience, we introduce $x^{(m,p)} = (\underbrace{2,\cdots,2}_{m-p},\underbrace{1,\cdots,1}_{2p})$, and denote $c(x^{(m,p)})$ as $c_{m,p}$. Note that

$$\begin{aligned} H^2\times\sum_{m+p}{}'\prod_{j=1}^{m-p}\varepsilon_{i_j}^2\prod_{j=m-p+1}^{m+p}\varepsilon_{i_j}\prod_{j=1}^{m+p} n_{i_j} =& \sum_{m+p+1}{}'\prod_{j=1}^{m-p+1}\varepsilon_{i_j}^2\prod_{j=m-p+2}^{m+p+1}\varepsilon_{i_j}\prod_{j=1}^{m+p+1} n_{i_j} + \sum_{m+p+2}{}'\prod_{j=1}^{m-p}\varepsilon_{i_j}^2\prod_{j=m-p+1}^{m+p+2}\varepsilon_{i_j}\prod_{j=1}^{m+p+2} n_{i_j}\\ &+ 4p\sum_{m+p+1}{}'\prod_{j=1}^{m-p+1}\varepsilon_{i_j}^2\prod_{j=m-p+2}^{m+p+1}\varepsilon_{i_j}\prod_{j=1}^{m+p+1} n_{i_j} + 2p(2p-1)\sum_{m+p}{}'\prod_{j=1}^{m-p+2}\varepsilon_{i_j}^2\prod_{j=m-p+3}^{m+p}\varepsilon_{i_j}\prod_{j=1}^{m+p} n_{i_j}\\ &+ \text{other terms}. \end{aligned} \tag{A9}$$

Here, "other terms" refer to the terms containing ε_i^3 or ε_i^4. Whereby, we derive the following recursive relation,

$$c_{m+1,p+1} = c_{m,p} + c_{m,p+1} + 4(p+1)c_{m,p+1} + (2p+4)(2p+3)c_{m,p+2}, \tag{A10}$$

using which one can prove that $c_{m,p} = \binom{m}{p}\frac{(2m-1)!!}{(2p-1)!!}$ by induction. Thus we obtain

$$\begin{aligned} \lim_{L\to\infty}\frac{\langle H^{2m}\rangle}{L^m} =& \sum_{p=1}^{2m}\sum_{\substack{x_1\geqslant\cdots\geqslant x_p\geqslant 1\\ |x|=2m}} c(x)\sum_{p}{}'\prod_{j=1}^{p}\varepsilon_{i_j}^{x_j}\left\langle\prod_{j=1}^{p} n_{i_j}\right\rangle = \sum_{p=1}^{2m}\sum_{\substack{x_1\geqslant\cdots\geqslant x_p\geqslant 1\\ |x|=2m}} c(x)\nu^p\lim_{L\to\infty}\frac{f(x)}{L^m}\\ =&(2m-1)!!\,\nu^m\sum_{p=0}^{m} c_{m,p}\lim_{L\to\infty}\frac{f(x^{(m,p)})}{L^m}. \end{aligned} \tag{A11}$$

To calculate $f(x^{(m,p)})$, first notice that

$$f(x^{(m+1,0)}) = f(x^{m,0})f(2) - mf(4,2,\cdots,2). \tag{A12}$$

Therefore we have

$$\lim_{L\to\infty}\frac{f(x^{(m+1,0)})}{L^{m+1}} = \sigma_\varepsilon^2\lim_{L\to\infty}\frac{f(x^{(m,0)})}{L^m} = \sigma_\varepsilon^{2(m+1)}. \tag{A13}$$

Furthermore, because

$$f(x^{(m,p+1)}) = f(\underbrace{2,\cdots 2}_{m-p-1},\underbrace{1,\cdots,1}_{2p+1})f(1) - (m-p-1)f(3,\underbrace{2,\cdots,2}_{m-p-2},\underbrace{1,\cdots,1}_{2p+1}) - (2p+1)f(x^{(m,p)}), \tag{A14}$$

we have

$$\lim_{L\to\infty}\frac{f(x^{(m,p+1)})}{L^m} = -(2p+1)\lim_{L\to\infty}\frac{f(x^{(m,p)})}{L^m} = (-1)^p(2p+1)!!\,\sigma_\varepsilon^{2m}. \tag{A15}$$

In summary, we obtain

$$\lim_{L\to\infty}\frac{\langle H^{2m}\rangle}{L^m} = (2m-1)!!\,\nu^m(1-\nu)^m\sigma_\varepsilon^{2m}. \tag{A16}$$

Let $\sigma_\varepsilon' = \sqrt{\nu(1-\nu)}\sigma_\varepsilon$, and then we have the expected results,

$$\lim_{L\to\infty}\left\langle\left(\frac{H}{\sqrt{L}\,\sigma_\varepsilon'}\right)^m\right\rangle = \begin{cases}0 & m \text{ is odd},\\ (m-1)!! & m \text{ is even}.\end{cases} \tag{A17}$$

Similarly,

$$\lim_{L\to\infty}\left\langle\left(\frac{Q}{\sqrt{L}\,\sigma_q'}\right)^m\right\rangle = \begin{cases}0 & m \text{ is odd},\\ (m-1)!! & m \text{ is even},\end{cases} \tag{A18}$$

where $\sigma_q' = \sqrt{\nu(1-\nu)}\sigma_q$.

Finally, we need to calculate $\langle H^m Q^n\rangle$. For the bivariate case, we first introduce the p-tuple of rank 2, given by $z = \binom{x}{y} = \binom{x_1 \quad \cdots \quad x_p}{y_1 \quad \cdots \quad y_p}$, where x_j, y_i are nonnegative integers and $x_j + y_j \geqslant 1$. Then the moment of z is given by

$$f(z) = \sum_p{}' \varepsilon_{i_1}^{x_1} q_{i_1}^{y_1}\, \varepsilon_{i_2}^{x_2} q_{i_2}^{y_2} \cdots\, \varepsilon_{i_p}^{x_p} q_{i_p}^{y_p}. \tag{A19}$$

Similarly, we have

$$f(z) = f\begin{pmatrix} x_1 & \cdots & x_{p-1} \\ y_1 & \cdots & y_{p-1} \end{pmatrix} f\begin{pmatrix} x_p \\ y_p \end{pmatrix} - \sum_{j=1}^{p-1} f\begin{pmatrix} x_1 & \cdots & x_j + x_p & \cdots & x_{p-1} \\ y_1 & \cdots & y_j + y_p & \cdots & y_{p-1} \end{pmatrix}, \tag{A20}$$

and therefore $\lim_{L\to\infty} f(z)L^{-|z|/2} = 0$ if $\max\{z\} = \max\{x_j + y_j\} \geqslant 3$, where $|z| = |x| + |y|$. Further, we have $\lim_{L\to\infty} f(z)L^{-|z|/2} = 0$ if $x_j = y_j = 1$ for some j. This is obvious for 1-tuple. Providing that it holds for $(p-1)$-tuple, for p-tuple z with $x_p = y_p = 1$, we have

$$f(z) = f\begin{pmatrix} x_1 & \cdots & x_{p-1} \\ y_1 & \cdots & y_{p-1} \end{pmatrix} f\begin{pmatrix} 1 \\ 1 \end{pmatrix} - \sum_{j=1}^{p-1} f\begin{pmatrix} x_1 & \cdots & x_j + 1 & \cdots & x_{p-1} \\ y_1 & \cdots & y_j + 1 & \cdots & y_{p-1} \end{pmatrix}. \tag{A21}$$

As $x_j + y_j + 1 \geqslant 3$, $\lim_{L\to\infty} f(z)L^{-|z|/2} = 0$ also holds true for p-tuple. This means that in the calculation of $\lim_{L\to\infty}\langle H^m Q^n\rangle L^{-(m+n)/2}$ only moment like

$$z = \begin{pmatrix} x & 0 \\ 0 & y \end{pmatrix} = \begin{pmatrix} \overbrace{2\cdots 2}^{p_1} & \overbrace{1\cdots 1}^{p_2} & 0\cdots 0 & 0\cdots 0 \\ 0\cdots 0 & 0\cdots 0 & \underbrace{2\cdots 2}_{p_3} & \underbrace{1\cdots 1}_{p_4} \end{pmatrix}, \tag{A22}$$

where $2p_1 + p_2 = m$ and $2p_3 + p_4 = n$. More importantly, one can easily prove that

$$\lim_{L\to\infty} \frac{1}{L^{|x|/2+|y|/2}} f\begin{pmatrix} x & 0 \\ 0 & y \end{pmatrix} = \lim_{L\to\infty} \frac{1}{L^{|x|/2}} f\begin{pmatrix} x \\ 0 \end{pmatrix} \lim_{L\to\infty} \frac{1}{L^{|y|/2}} f\begin{pmatrix} 0 \\ y \end{pmatrix}. \tag{A23}$$

This means that the nonvanishing terms in $\lim_{L\to\infty}\langle H^m Q^n\rangle L^{-(m+n)/2}$ are just all the product of the nonvanishing terms in $\lim_{L\to\infty}\langle H^m\rangle L^{-m/2}$ and $\lim_{L\to\infty}\langle Q^n\rangle L^{-n/2}$. Therefore we obtain

$$\lim_{L\to\infty} \left\langle \left(\frac{H}{\sqrt{L}\,\sigma'_\varepsilon}\right)^m \left(\frac{Q}{\sqrt{L}\,\sigma'_q}\right)^n \right\rangle = \lim_{L\to\infty} \left\langle \left(\frac{H}{\sqrt{L}\,\sigma'_\varepsilon}\right)^m \right\rangle \lim_{L\to\infty} \left\langle \left(\frac{Q}{\sqrt{L}\,\sigma'_q}\right)^n \right\rangle. \tag{A24}$$

Hence, $H/(\sqrt{L}\sigma'_\varepsilon)$ and $Q/(\sqrt{L}\sigma'_q)$ are two independent normal distribution. When $\lim_{L\to\infty} \frac{1}{L}\sum_{i=1}^{L} \varepsilon_i q_i \neq 0$, $H/(\sqrt{L}\sigma'_\varepsilon)$ and $Q/(\sqrt{L}\sigma'_q)$ form a bivariate normal distribution. This conclusion can be generalized to multivariate cases easily.

APPENDIX B: CENTRAL LIMIT THEOREM FOR INTERACTING FERMIONS

The single-particle part of the interacting Hamiltonian can be expressed by

$$H_0 = \sum_{i,j} t_{ij} c_i^\dagger c_j = \sum_i \varepsilon_i f_i^\dagger f_j, \tag{B1}$$

where f_j is the annihilation operator of the eigenstate of H_0. Furthermore, we also need ε_i to be bounded by some positive number M in addition to Eq. (A2). For the interaction part, we only consider the nearest-neighbor (NN) interaction for simplicity, which is given by

$$S = \sum_i n_i n_{i+1} = \sum_i c_{i+1}^\dagger c_i^\dagger c_i c_{i+1} = \sum_{ijkl} S_{ijkl} f_i^\dagger f_j^\dagger f_k f_l. \tag{B2}$$

Hence, the interacting Hamiltonian is given by

$$H = H_0 + US, \tag{B3}$$

where U is the interaction strength.

Let us first calculate $\langle S\rangle$, $\langle S^2\rangle$, and $\langle S^3\rangle$. After some algebra, we obtain

$$\begin{aligned} &\langle S\rangle = L\langle 2\rangle, \quad \langle S^2\rangle = L\langle 2\rangle + 2L\langle 3\rangle + L(L-3)\langle 4\rangle, \\ &\langle S^3\rangle = L\langle 2\rangle + 6L\langle 3\rangle + 3L(L-1)\langle 4\rangle + 6L(L-4)\langle 5\rangle + L(L-5)(L-6)\langle 6\rangle. \end{aligned} \tag{B4}$$

As $\lim_{L\to\infty}\langle S\rangle/(\nu N)=1$, we consider the moments of $\frac{S-\nu N}{\sqrt{L}}$ and $\frac{H-\nu UN}{\sqrt{L}}$ in analogy to the noninteracting CLT. Utilizing Eq. (B4), we have

$$\frac{1}{L}\langle(S-\nu N)^2\rangle = \langle 2\rangle + 2\langle 3\rangle - 3\langle 4\rangle + L(\langle 4\rangle - 2\nu^2\langle 2\rangle + \nu^4), \tag{B5}$$

$$\begin{aligned}\frac{1}{L}\langle(S-\nu N)^3\rangle &= \langle 2\rangle + 6\langle 3\rangle + 3(L-1)\langle 4\rangle + 6(L-4)\langle 5\rangle + (L-5)(L-6)\langle 6\rangle + 3\nu^4L^2\langle 2\rangle - \nu^6L^2 - 3\nu^2L(\langle 2\rangle + 2\langle 3\rangle \\ &\quad + (L-3)\langle 4\rangle) \\ &= L[-9(\langle 6\rangle - \nu^2\langle 4\rangle) + 6(\langle 5\rangle - \nu^2\langle 3\rangle) + 3(\langle 4\rangle - \nu^2\langle 2\rangle)] + L^2(\langle 6\rangle - 3\nu^2\langle 4\rangle + 3\nu^4\langle 2\rangle - \nu^6) + \text{Constant}.\end{aligned} \tag{B6}$$

Using the exact expression of $\langle p\rangle$, it is readily to prove

$$\lim_{L\to\infty}\left\langle\left(\frac{S-\nu N}{\sqrt{L}}\right)^2\right\rangle = \nu^2(1-\nu)^2, \quad \lim_{L\to\infty}\left\langle\left(\frac{S-\nu N}{\sqrt{L}}\right)^3\right\rangle = 0. \tag{B7}$$

Although we just analytically compute the first three moments of $\frac{S-\nu N}{\sqrt{L}}$, the numerical result fits normal distribution very well up to the fifth moment.

Next, we need to calculate $\langle HS^m\rangle$. First, consider the following operator:

$$O = \sum_i \prod_{j=1}^{p} n_{i+i_j}, \tag{B8}$$

where $i_1 < i_2 < \cdots < i_p$ are some fixed integers. Thus we can derive

$$\begin{aligned}\langle HO\rangle &= \sum_k t_{kk}\left\langle n_k\prod_{j=1}^{p} n_{i+i_j}\right\rangle \\ &= \sum_i\sum_{k=1}^{p} t_{i+i_k,i+i_k}\left\langle\prod_{j=1}^{p} n_{i+i_j}\right\rangle + \sum_i\sum_{k\neq i+i_1,i+\cdots,i_p} t_{kk}\left\langle n_k\prod_{j=1}^{p} n_{i+i_j}\right\rangle \\ &= \langle p\rangle\sum_i\sum_{k=1}^{p} t_{i+i_k,i+i_k} + \langle p+1\rangle\sum_i\sum_i\sum_{k\neq i+i_1,i+\cdots,i_p} t_{kk} \\ &= p\langle p\rangle\sum_k t_{kk} + (L-p)\langle p+1\rangle\sum_k t_{kk} = L\langle p\rangle\nu\sum_k t_{kk} = \langle H\rangle\langle O\rangle,\end{aligned} \tag{B9}$$

where $(L-p)\langle p+1\rangle = (N-p)\langle p\rangle$ is used. As S^m is just the sum of different O's, we have $\langle HS^m\rangle = \langle H\rangle\langle S^m\rangle$. Consequently, we obtain $\langle H(S-\nu N)^m\rangle = \langle H\rangle\langle(S-\nu N)^m\rangle$.

Another term we need to evaluate is $\langle H^2(S-\nu N)\rangle$. It is more convenient to compute this term in the eigenstate basis,

$$\langle H^2(S-\nu N)\rangle = \langle H^2S\rangle - \nu N\langle H^2\rangle = \sum_{i,j}{}' S_{ij}\langle H^2\tilde{n}_i\tilde{n}_j\rangle - \nu N\langle H^2\rangle, \tag{B10}$$

where $S_{ij} = S_{ijji} - S_{ijij}$ and $\tilde{n}_i = f_i^\dagger f_i$. Therefore we have

$$\langle H^2S\rangle = \langle 4\rangle\sum_{i,j,k,l}{}' S_{ij}\varepsilon_k\varepsilon_l + \langle 3\rangle\sum_{i,j,k}{}' S_{ij}\varepsilon_k(2\varepsilon_i + 2\varepsilon_j + \varepsilon_k) + \langle 2\rangle\sum_{i,j}{}' S_{ij}(\varepsilon_i+\varepsilon_j)^2. \tag{B11}$$

For the third term, we have

$$\left|\sum_{i,j}{}' S_{ij}(\varepsilon_i+\varepsilon_j)^2\right| \leqslant 4M^2\sum_{i,j}{}' S_{ij} = O(L), \tag{B12}$$

where we used $S_{ij} \geqslant 0$ because S is positive semidefinite, and $\sum'_{i,j} |S_{ij}|\langle 2\rangle = \langle S\rangle = L\langle 2\rangle$. For the second term, we have

$$\begin{aligned}\sum_{i,j,k}{}' S_{ij}\varepsilon_k(2\varepsilon_i + 2\varepsilon_j + \varepsilon_k) &= \sum_{i,j}{}' S_{ij}\sum_k \varepsilon_k^2 - \sum_{i,j}{}' S_{ij}\left(\varepsilon_i^2 + \varepsilon_j^2\right) + 2\sum_{i,j}{}' S_{ij}(\varepsilon_i + \varepsilon_j)\sum_k \varepsilon_k - 2\sum_{i,j}{}' S_{ij}(\varepsilon_i + \varepsilon_j)^2 \\ &= L\sum_k \varepsilon_k^2 + O(L) + O(L)\sum_k \varepsilon_k. \end{aligned} \tag{B13}$$

For the first term, we have

$$\begin{aligned}\sum_{i,j,k,l}{}' S_{ij}\varepsilon_k\varepsilon_l &= \sum_{i,j,k}{}' S_{ij}\varepsilon_k\sum_l \varepsilon_l - \sum_{i,j,k}{}' S_{ij}\varepsilon_k(\varepsilon_i + \varepsilon_j + \varepsilon_k) \\ &= \sum_{i,j}{}' S_{ij}\left(\sum_k \varepsilon_k\right)^2 - \sum_{i,j}{}' S_{ij}(\varepsilon_i + \varepsilon_j)\sum_l \varepsilon_l - \sum_{i,j}{}' S_{ij}\sum_k \varepsilon_k^2 + O(L) + O(L)\sum_k \varepsilon_k \\ &= L\left(\sum_k \varepsilon_k\right)^2 - L\sum_k \varepsilon_k^2 + O(L) + O(L)\sum_k \varepsilon_k. \end{aligned} \tag{B14}$$

In conclusion, we obtain

$$\begin{aligned}\langle H^2 S\rangle = \langle 4\rangle L\left(\sum_k \varepsilon_k\right)^2 + (\langle 3\rangle - \langle 4\rangle)L\sum_k \varepsilon_k^2 \\ + O(L) + O(L)\sum_k \varepsilon_k, \end{aligned} \tag{B15}$$

$$\nu\langle H^2\rangle = \langle 2\rangle\left(\sum_k \varepsilon_k\right)^2 + (\langle 1\rangle - \langle 2\rangle)\sum_k \varepsilon_k^2. \tag{B16}$$

Thus we have

$$\lim_{L\to\infty} \frac{\langle H^2(S - \nu N)\rangle}{L^{3/2}} = 0. \tag{B17}$$

With all these properties, we can calculate up to the third moment of $\frac{H-\nu UN}{\sqrt{L}}$, which is given by

$$\begin{aligned}\lim_{L\to\infty}\left\langle\left(\frac{H - \nu UN}{\sqrt{L}}\right)^2\right\rangle &= \sigma_\varepsilon^2\nu(1-\nu) + U^2\nu^2(1-\nu)^2, \\ \lim_{L\to\infty}\left\langle\left(\frac{H - \nu UN}{\sqrt{L}}\right)\right\rangle &= \lim_{L\to\infty}\left\langle\left(\frac{H - \nu UN}{\sqrt{L}}\right)^3\right\rangle = 0. \end{aligned} \tag{B18}$$

Note that ED in small systems finds the prominent asymmetry of the DOS, signified by a finite third moment. However, we prove that the third moment actually goes to zero in the thermodynamic limit, suggesting that the asymmetry of the spectrum is reduced even without an exact symmetry. Notwithstanding, an exactly symmetric DOS dictates that all odd-order moments are zero, so a vanishing third moment is not enough to prove that the spectrum is exactly symmetric.

APPENDIX C: SPECTRAL FORM FACTOR

To further investigate the spectral properties of the quasiperiodic systems, we study the spectral form factor (SFF)

$$K(t) = \frac{1}{D}\langle|\mathrm{tr}U(t)|^2\rangle_{\text{ensemble}}, \tag{C1}$$

where $U(t) = e^{-itH}$ is the evolution operator, and $\langle\cdot\rangle_{\text{ensemble}}$ denotes the ensemble average. The SFF is constant $K(t) = 1$ for the Poisson distribution, while the analytic form of the SFF of the GOE is

$$K(\tau) = \begin{cases} 2\tau - \tau\ln(2\tau+1), & \tau < 1 \\ 2 - \tau\ln\frac{2\tau+1}{2\tau-1}, & \tau \leqslant 1 \end{cases}, \tag{C2}$$

where $\tau = t/t_H$ and t_H is the Heisenberg time. If the density of state (DOS) is constant ρ, then $t_H = 2\pi/\rho$. Generally, the SFF contains more information than the mean gap ratio. However, as the SFF is not self-averaging, a considerable number of realizations are necessary to obtain a meaningful result. This is exceptionally complicated in the quasiperiodic systems, because quasiperiodic systems are deterministic and have at most one independent random variable, the random phase. To overcome this difficulty, we utilize the time average technique to reduce the fluctuation. The time-averaged SFF is defined

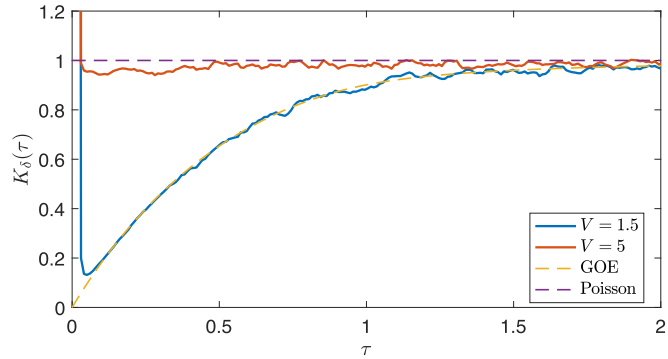

FIG. 5. The time-averaged SFF of the t_1-t_2 model with LR interaction and $U = 1$. The results are calculated in the $L = 16$ system and averaged over 100 random phases. Additionally, we use 2000 eigenvalues in the middle of the spectrum and choose $\delta = 1/20$ for the time averaging.

as [42]

$$K_\delta(\tau) = \frac{1}{\delta}\int_{\tau-\delta/2}^{\tau+\delta/2} K(t)\mathrm{d}\tau, \tag{C3}$$

where we choose $\delta = 1/20$ in our calculation. In Fig. 5, we calculate the SFF for the t_1-t_2 model with LR interaction of length $L = 16$. Further, we choose $D = 2000$ states in the middle of the spectrum to guarantee an almost constant DOS. Deep in the thermal or MBL phase, Fig. 5 shows that the SFF agrees excellently with the random matrix theory. Furthermore, we have checked the SFF in the AA, and Anderson models with either LR or SR interaction, and all of them work very well deep in the thermal or MBL phase.

[1] P. W. Anderson, Absence of diffusion in certain random lattices, Phys. Rev. **109**, 1492 (1958).

[2] R. Nandkishore and D. A. Huse, Many-body localization and thermalization in quantum statistical mechanics, Annu. Rev. Condens. Matter Phys. **6**, 15 (2015).

[3] E. Altman and R. Vosk, Universal dynamics and renormalization in many-body-localized systems, Annu. Rev. Condens. Matter Phys. **6**, 383 (2015).

[4] J. Z. Imbrie, On many-body localization for quantum spin chains, J. Stat. Phys. **163**, 998 (2016).

[5] J. Z. Imbrie, Diagonalization and many-body localization for a disordered quantum spin chain, Phys. Rev. Lett. **117**, 027201 (2016).

[6] D. A. Abanin, E. Altman, I. Bloch, and M. Serbyn, *Colloquium:* Many-body localization, thermalization, and entanglement, Rev. Mod. Phys. **91**, 021001 (2019).

[7] S. Gopalakrishnan and S. Parameswaran, Dynamics and transport at the threshold of many-body localization, Phys. Rep. **862**, 1 (2020).

[8] S. Das Sarma, A. Kobayashi, and R. E. Prange, Proposed experimental realization of Anderson localization in random and incommensurate artificially layered systems, mobility edges, Phys. Rev. Lett. **56**, 1280 (1986).

[9] S. Das Sarma, S. He, and X. C. Xie, Mobility edge in a model one-dimensional potential, mobility edges, Phys. Rev. Lett. **61**, 2144 (1988).

[10] D. J. Thouless, Localization by a potential with slowly varying period, mobility edges, Phys. Rev. Lett. **61**, 2141 (1988).

[11] J. Biddle and S. Das Sarma, Predicted mobility edges in one-dimensional incommensurate optical lattices: An exactly solvable model of Anderson localization, Phys. Rev. Lett. **104**, 070601 (2010).

[12] J. Biddle, D. J. Priour, B. Wang, and S. Das Sarma, Localization in one-dimensional lattices with non-nearest-neighbor hopping: Generalized Anderson and Aubry-André models, Phys. Rev. B **83**, 075105 (2011).

[13] S. Ganeshan, J. Pixley, and S. Das Sarma, Nearest neighbor tight binding models with an exact mobility edge in one dimension, Phys. Rev. Lett. **114**, 146601 (2015).

[14] X. Li, X.-P. Li, and S. Das Sarma, Mobility edges in one-dimensional bichromatic incommensurate potentials, Phys. Rev. B **96**, 085119 (2017).

[15] X. Li and S. Das Sarma, Mobility edge and intermediate phase in one-dimensional incommensurate lattice potentials, mobility edges, Phys. Rev. B **101**, 064203 (2020).

[16] Y. Wang, X. Xia, L. Zhang, H. Yao, S. Chen, J. You, Q. Zhou, and X.-J. Liu, One-dimensional quasiperiodic mosaic lattice with exact mobility edges, Phys. Rev. Lett. **125**, 196604 (2020).

[17] I. V. Gornyi, A. D. Mirlin, and D. G. Polyakov, Interacting electrons in disordered wires: Anderson localization and low-t transport, Phys. Rev. Lett. **95**, 206603 (2005).

[18] D. Basko, I. Aleiner, and B. Altshuler, Metal–insulator transition in a weakly interacting many-electron system with localized single-particle states, Ann. Phys. **321**, 1126 (2006).

[19] J. A. Kjäll, J. H. Bardarson, and F. Pollmann, Many-body localization in a disordered quantum ising chain, Phys. Rev. Lett. **113**, 107204 (2014).

[20] D. J. Luitz, N. Laflorencie, and F. Alet, Many-body localization edge in the random-field Heisenberg chain, Phys. Rev. B **91**, 081103(R) (2015).

[21] I. Mondragon-Shem, A. Pal, T. L. Hughes, and C. R. Laumann, Many-body mobility edge due to symmetry-constrained dynamics and strong interactions, Phys. Rev. B **92**, 064203 (2015).

[22] X. Li, S. Ganeshan, J. H. Pixley, and S. Das Sarma, Many-body localization and quantum nonergodicity in a model with a single-particle mobility edge, Phys. Rev. Lett. **115**, 186601 (2015).

[23] T. Devakul and R. R. Singh, Early breakdown of area-law entanglement at the many-body delocalization transition, Phys. Rev. Lett. **115**, 187201 (2015).

[24] S. Nag and A. Garg, Many-body mobility edges in a one-dimensional system of interacting Fermions, Phys. Rev. B **96**, 060203(R) (2017).

[25] B. Villalonga, X. Yu, D. J. Luitz, and B. K. Clark, Exploring one-particle orbitals in large many-body localized systems, Phys. Rev. B **97**, 104406 (2018).

[26] X. Wei, C. Cheng, X. Gao, and R. Mondaini, Investigating many-body mobility edges in isolated quantum systems, Phys. Rev. B **99**, 165137 (2019).

[27] T. Chanda, P. Sierant, and J. Zakrzewski, Many-body localization transition in large quantum spin chains: The mobility edge, Phys. Rev. Res. **2**, 032045(R) (2020).

[28] X. Wei, R. Mondaini, and X. Gao, Characterization of many-body mobility edges with random matrices, arXiv:2001.04105.

[29] R. Yousefjani and A. Bayat, Mobility edge in long-range interacting many-body localized systems, Phys. Rev. B **107**, 045108 (2023).

[30] W. De Roeck, F. Huveneers, M. Müller, and M. Schiulaz, Absence of many-body mobility edges, Phys. Rev. B **93**, 014203 (2016).

[31] A. Morningstar, L. Colmenarez, V. Khemani, D. J. Luitz, and D. A. Huse, Avalanches and many-body resonances in many-body localized systems, Phys. Rev. B **105**, 174205 (2022).

[32] Y.-T. Tu, D. Vu, and S. Das Sarma, Localization spectrum of a bath-coupled generalized Aubry-André model in the presence of interactions, Phys. Rev. B **108**, 064313 (2023).

[33] T. Kohlert, S. Scherg, X. Li, H. P. Lüschen, S. Das Sarma, I. Bloch, and M. Aidelsburger, Observation of many-body localization in a one-dimensional system with a single-particle mobility edge, Phys. Rev. Lett. **122**, 170403 (2019).

[34] K. Huang, D. Vu, X. Li, and S. Das Sarma, Incommensurate many-body localization in the presence of long-range hopping and single-particle mobility edge, Phys. Rev. B **107**, 035129 (2023).

[35] R. Lefèvre, K. Zawadzki, and G. Ithier, Many body density of states of a system of non interacting spinless fermions, New J. Phys. **25**, 063004 (2023).

[36] D. Vu, K. Huang, X. Li, and S. Das Sarma, Fermionic many-body localization for random and quasiperiodic systems in the presence of short- and long-range interactions, Phys. Rev. Lett. **128**, 146601 (2022).

[37] V. Oganesyan and D. A. Huse, Localization of interacting fermions at high temperature, Phys. Rev. B **75**, 155111 (2007).

[38] Y. Y. Atas, E. Bogomolny, O. Giraud, and G. Roux, Distribution of the ratio of consecutive level spacings in random matrix ensembles, Phys. Rev. Lett. **110**, 084101 (2013).

[39] G. De Tomasi, D. Hetterich, P. Sala, and F. Pollmann, Dynamics of strongly interacting systems: From fock-space fragmentation to many-body localization, Phys. Rev. B **100**, 214313 (2019).

[40] Z.-C. Yang, F. Liu, A. V. Gorshkov, and T. Iadecola, Hilbert-space fragmentation from strict confinement, Phys. Rev. Lett. **124**, 207602 (2020).

[41] S. N. Ethier, *The Doctrine of Chances: Probabilistic Aspects of Gambling* (Springer, Berlin, 2010).

[42] R. E. Prange, The spectral form factor is not self-averaging, Phys. Rev. Lett. **78**, 2280 (1997).